scientific data



DATA DESCRIPTOR

OPEN Dataset for Fracture and Impact **Toughness of High-Entropy Alloys**

Xuesong Fan¹, Shiyi Chen¹, Baldur Steingrimsson (1,2), Qingang Xiong³, Weidong Li¹⊠ & Peter K. Liaw^{1⊠}

Fracture dictates the service limits of metallic structures. Damage tolerance of materials may be characterized by fracture toughness rigorously developed from fracture mechanics, or less rigorous yet more easily obtained impact toughness (or impact energy as a variant). Given the promise of highentropy alloys (HEAs) in structural and damage-tolerance applications, we compiled a dataset of fracture toughness and impact toughness/energy from the literature till the end of the 2022 calendar year. The dataset is subdivided into three categories, i.e., fracture toughness, impact toughness, and impact energy, which contain 153, 14, and 78 distinct data records, respectively. On top of the alloy chemistry and measured fracture quantities, each data record also documents the factors influential to fracture. Examples are material-processing history, phase structures, grain sizes, uniaxial tensile properties, such as yield strength and elongation, and testing conditions. Data records with comparable conditions are graphically visualized by plots. The dataset is hosted in Materials Cloud, an open data repository.

Background & Summary

High-entropy alloys (HEAs) are one of the hottest fields of study in materials science in the recent decade¹⁻³. These alloys draw the attention of researchers in both academia and industry across the world because they revolutionize the traditional way of alloy design in multi-component alloy systems. To appreciate the revolution brought about by HEAs, one needs to first examine their definition. Though there is no a universally agreed-on definition existing, the seminal paper by Yeh, et al.4 define them as alloys containing at least 5 elements with concentrations between 5 and 35 atomic percent. It is clear from the definition that HEAs mainly disrupt multi-component alloys. In other words, low-order systems, i.e., quaternary, ternary, and binary alloys and pure metals, are not much impacted by the concept. It is straightforward to appreciate that mixing multiple elements is essential to the design of multicomponent alloys. However, the traditional and high-entropy ways of mixing are distinct. In the traditional way, there is always one component that is dominantly higher than the rest, although there may be up to 3 other components having concentrations greater than 5 atomic percent. The dominant component is termed the solvent and the remaining is the solutes. Ni-based superalloys (e.g., HAYNES® 282®) are perfect examples of this type. In the high-entropy way of mixing, there may be 2 or more components having dominance in concentration 1,2,4,5. For example, all the 5 elements in the Cantor alloy, i.e., CoCrFeMnNi⁵ have the equal dominance. Accordingly, the unambiguous identifications of the solvent and solutes in HEAs are often

The high-entropy way of mixing multiple components has led to several distinctive characteristics to the alloys made thereby. First, it induces high configurational entropy in alloys, according to the equation of the configurational entropy of mixing for ideal solid solutions, $\Delta S_{\text{mix,ideal}} = -R\sum_{i=1}^{n} c_i \ln(c_i)$, where R is the gas constant, c_i is the molar fraction of the ith component, and n is the total number of the constituent elements^{2,6}. Second, alloys are stabilized to simpler phase structures than the traditional way of mixing, according to the equation of the free energy of mixing, $\Delta G_{\rm mix} = \Delta H_{\rm mix} - T\Delta S_{\rm mix}$, where $\Delta H_{\rm mix}$ is the enthalpy of mixing 1,2,6. Therefore, single-phase solid solutions are very likely to form. Third, an abundance of elements dissolved in a solid solution result in a greater degree of lattice distortion, and thus strengthening, than ever before². Sluggish diffusion⁷, cocktail effect⁸, chemical short-range ordering⁹, and chemical fluctuation¹⁰ are other attributes differentiating HEAs from their traditional counterparts.

¹Department of Materials Science and Engineering, The University of Tennessee, Knoxville, TN, 37996, USA. ²Imagars LLC, Hillsboro, OR, 97124, USA. ³State Key Laboratory of Pulp and Paper Engineering, South China University of Technology, Guangzhou, 510640, China. [™]e-mail: wli20@utk.edu; pliaw@utk.edu

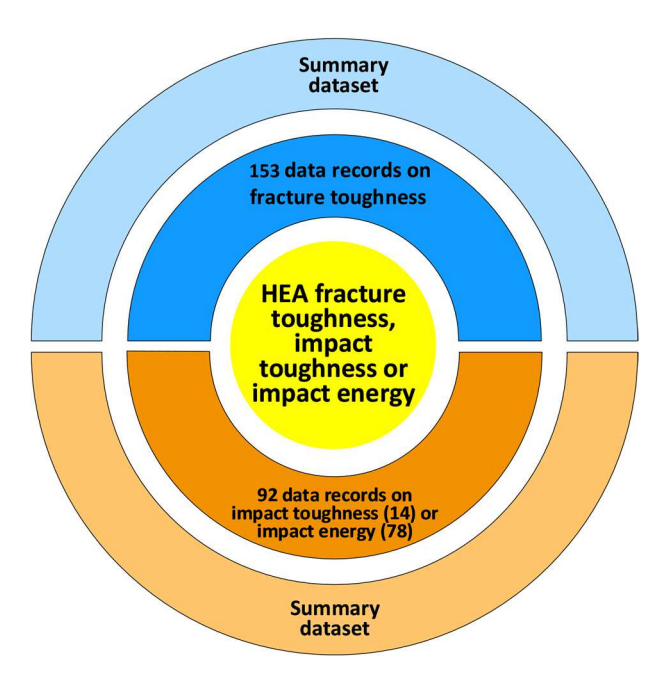


Fig. 1 Schematic structure of the database for the fracture, impact toughness and impact energy of the high-entropy alloys, which is comprised of 153 data records for the fracture toughness, 14 data records for the impact toughness, and 78 data records on the impact energy, with each record further constituted by an extended summary covering conditions from processing all the way to testing of the fracture toughness, the impact toughness, or the impact energy.

It is continually reported that these effects contribute, in part, to the unique deformation mechanisms mediated by dislocation dynamics¹¹, nano-twining¹², stacking faults¹³, and phase transformation¹⁴, as well as remarkable mechanical properties, such as strength-ductility balance, excellent fracture and fatigue resistance^{15–17} in HEAs. Among various mechanical properties, fracture toughness is one of the most fundamental yet critical properties dictating the feasibility of these alloy in engineering applications^{15,18}. It is simply because fracture toughness governs damage tolerance of materials in service. The reported fracture toughness of HEAs is rather scattered. In general, face-centered-cubic (fcc) alloys possess high fracture toughness whereas body-centered-cubic alloys are low¹⁵. Alloys with mixed or complex phase structures could exhibit fracture toughness ranging from low to high values depending on operative deformation mechanisms^{2,15}. Another quantity closely related to fracture toughness is impact toughness or impact energy^{2,15}, which is an older means of characterizing a material's resistance to impact loads using Charpy or Izod impact tests¹⁹.

Given the importance of the fracture toughness and impact toughness of HEAs in shaping their potential applications, we believe that it is important to make a compilation of them. Such a compilation can bring two major benefits. First, associating materials, processing histories, microstructures, and testing conditions of HEAs with their fracture toughness and impact toughness and compiling them in one dataset allows researchers to examine various patterns, gaining insights in devising new compositions or processing routes for improved fracture resistance. Second, the compiled data, especially if evolving over time, are instrumental to applying artificial intelligence (AI) and machine learning (ML) to finding HEAs of more fracture resistance. The present work is conceived in consideration of these benefits.

Methods

Fracture toughness reflects a material's resistance to crack propagation. It is the critical stress intensity factor of a sharp crack where the propagation of a crack suddenly becomes unstable. The value of fracture toughness is affected by the constraint conditions at the tip of a crack, namely, the thickness of the component. Thin components impose less constraints onto the crack tip and induce plane-stress conditions. On the other hand, thick components impose more constraints and cause plane-strain conditions. For a given material, as the thickness of the component increases, its fracture toughness will first rise and then decline until reaching a steady value, which will not change much with a further increase in thickness. This lowest steady value is characteristic of the material and is deemed an intrinsic material property, known as plane-strain fracture toughness, K_{IC}^{-19} . Under the non-plane-strain condition, fracture toughness is not regarded a material property and designated K_C .

American Society for Testing and Materials (ASTM) standardizes the measurement of K_{IC} in its standard ASTM E399²⁰. The measurement starts with measuring a conditional plane-strain fracture toughness K_Q . Then, K_Q is checked against several validity requirements. If all validity checks are passed, K_Q is a valid K_{IC} . If any of the validity requirements cannot be met, K_Q will stay conditional. One limitation of the fracture toughness measurement with ASTM E399 is that it is based on Linear Elastic Fracture Mechanics and thus only applicable to materials that are brittle or have very limited plasticity, which can ensure a small plastic zone size and K-dominance at the crack tip. For ductile materials, sample sizes may need to be impractically large in order for Linear Elastic

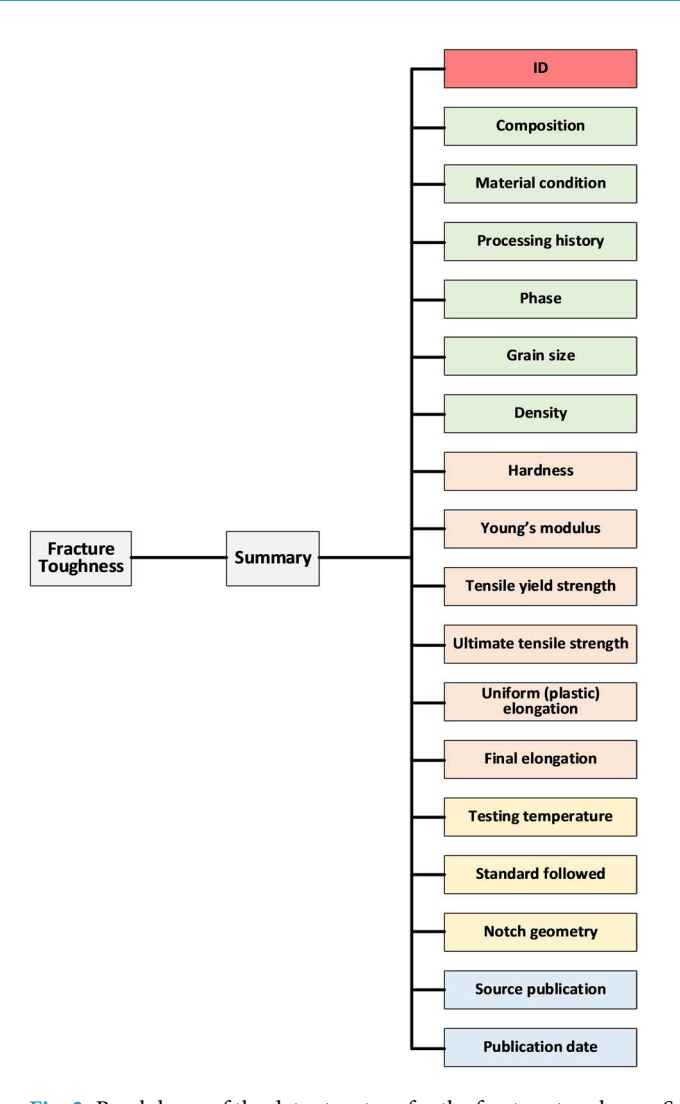


Fig. 2 Breakdown of the data structure for the fracture toughness. Summary is categorized by color.

Fracture Mechanics and K_{IC} measurements to be valid. As a result, it is extremely difficult or almost unlikely to obtain valid K_{IC} measurements for ductile materials with ASTM E399. In this case, ASTM E1820 based on the J-integral concept is usually used ^{19,21}. J-integral calculates the strain energy release rate, i.e., energy release per unit fracture surface area during crack propagation, in a material. Like ASTM E399, ASTM E1820 first measured a conditional critical J-integral, J_Q . J_Q is then check against a series of validity requirements. If all met, J_Q is deemed a valid critical fracture energy, J_{IC} . J_{IC} can be used as is to characterize a material's resistance to crack propagation. Or it can be converted to K_{IC} with ^{2,15,19}

$$K_{IC} = \sqrt{J_{IC}E'}, \qquad (1)$$

where E' is the effective Young's modulus, which equals E in plane-stress conditions and $E/(1-v^2)$ in plane-strain conditions, where E and v are Young's modulus and Poisson's ratio of the material, respectively.

Prior to the appearance of fracture mechanics as a rigorous discipline, pendulum-type impact tests, e.g., Charpy and Izod impact tests, are common ways to characterize the resistance of materials to fracture by impact loads. When a pendulum is released from a given height and impact the notched sample to fracture, and eventually swing to a peak height that is lower than the release height, certain energy is absorbed by the material in the form of mechanical work and this absorbed energy equals the potential energy difference of the pendulum at the beginning and ending heights. The absorbed energy is a measure of the material's notch toughness. Although this type of test fails to measure intrinsic material properties and the measurements can only be used for comparative or ranking purposes, they are still popular in modern uses given the ease and low cost of operations. ASTM E23²² and ASTM E2248²³ standardize impact testing of standard-sized notched bars and miniaturized Charpy V-notch specimens.

The first publication on fracture toughness of HEAs appeared in 2013, which used a non-standard nanoin-dentation method to measure the fracture toughness of the FeCoNiCrCuTiMoAlSiB_{0.5} alloy²⁴. One year later, in 2014, the measurements with ASTM-E399 were made on the AlCoCrCuFeNi alloy by Roy *et al.*²⁵. This first

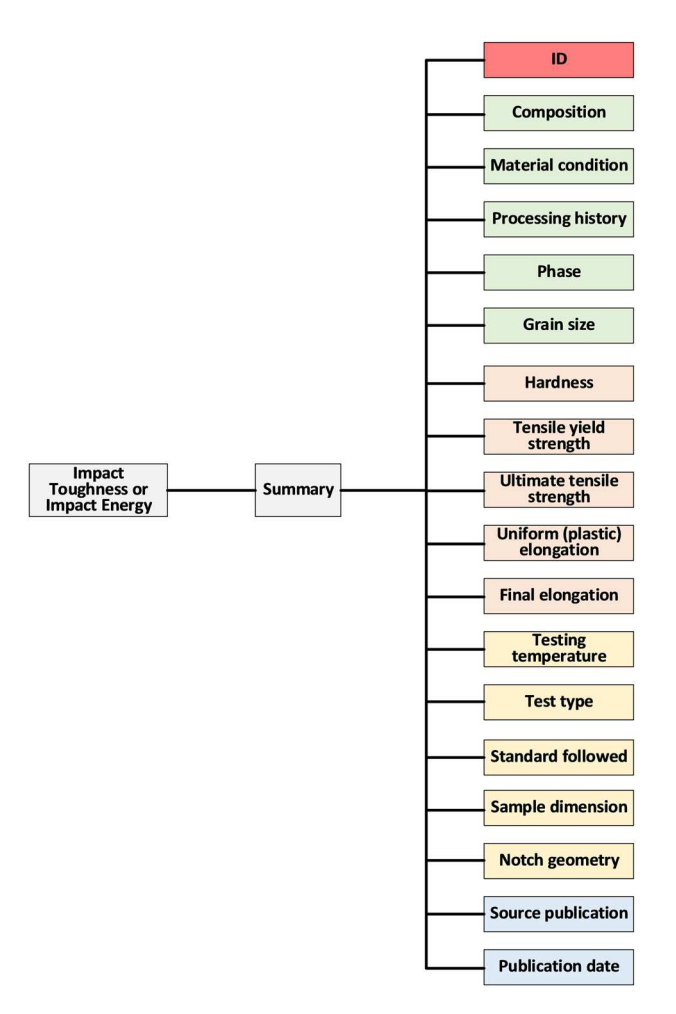


Fig. 3 Breakdown of the data structures for the impact toughness and the impact energy.

publication on using impact testing to characterize the impact energy of HEAs is on a series of Al_x CoCrFeNi alloy in 2016^{26} .

The data on the fracture toughness and impact energy in the present dataset are sourced through the publications from the appearance of the very first publications until the end of the 2022 calendar year. Web of Science and Google Scholar were two of the main search engines used for searching. Following downloading the publications, figures therein containing fracture toughness and impact energy data were screenshotted. The data points of the screenshots were digitized with WebPlotDigitizer version 4.5²⁷ and deposited in an Excel template. Alongside, the composition, processing history, microstructure (phase structure and grain size) hardness, uniaxial tensile properties (strengths and elongations), testing conditions (temperature, test type, etc.), and references are recorded, when available in the same publication or related publications by the same research group. We intentionally refrain us from extracting the data from vastly different publications to avert any misleading, as the conditions of the same material may be significantly different among publications by different research groups. Accordingly, some fields of a given material may not have valid values, and they are filled with NA.

Additionally, the raw data in the literature may be reported in varied units. Unit conversions are applied to the data extracted, so that the data in the dataset have consistent units. For impact tests, some publication report impact energies, while others normalized the energy by the fractured surface area and termed it impact toughness. To maintain consistency, we opt to separate them out into two sub-datasets, one for impact energy and the other for impact toughness.

Data Records

The data is saved in four worksheets of a Microsoft Excel workbook. The four worksheets are "Front page", "Fracture toughness", "Impact toughness", and "Impact energy". The Excel dataset is archived in the open-access data repository, Materials Cloud (URL: https://www.materialscloud.org/), for ready access²⁸. It companions our published HEA fatigue dataset^{29,30}.

All data in the Excel repository are subdivided into three broad categories based on the types of fracture tests conducted and the values reported, that is, fracture toughness, impact toughness, and impact energy. The three categories comprise 153, 14, and 78 data records, respectively, as schematically illustrated in Fig. 1. Each

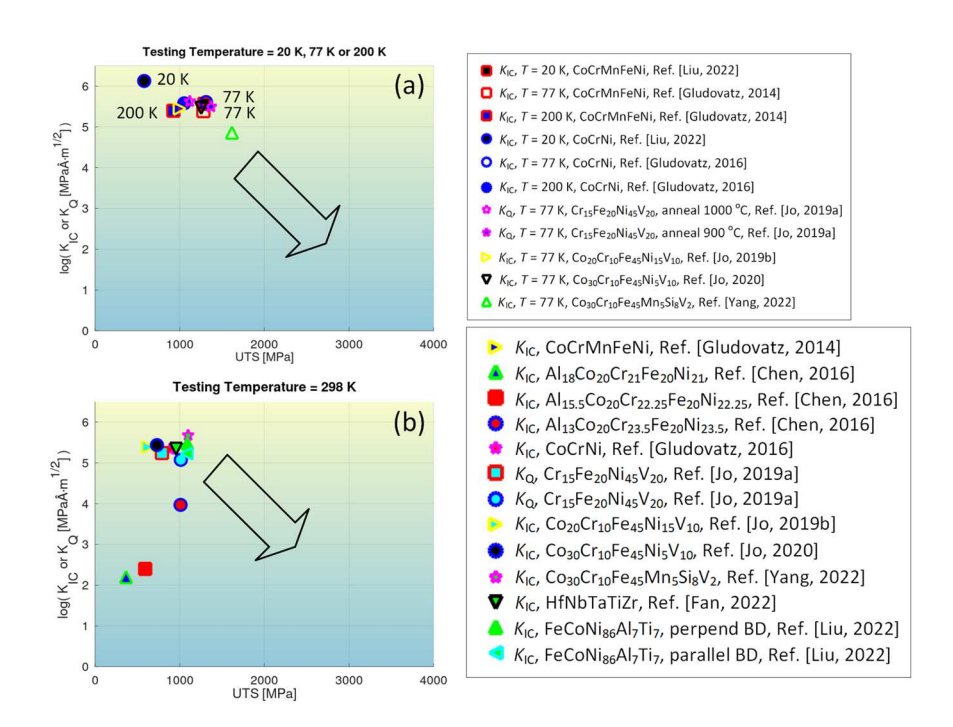


Fig. 4 Graphical compilation of K_{IC} or K_Q of high-entropy alloys as a function of their ultimate tensile strengths at different testing temperatures $^{62-71}$. (a) T=20K, 77 K, or 200 K. (b) T=298 K. Note that only a fraction of data in the dataset with ultimate tensile strength available is plotted. The arrows in the graph indicate a trend.

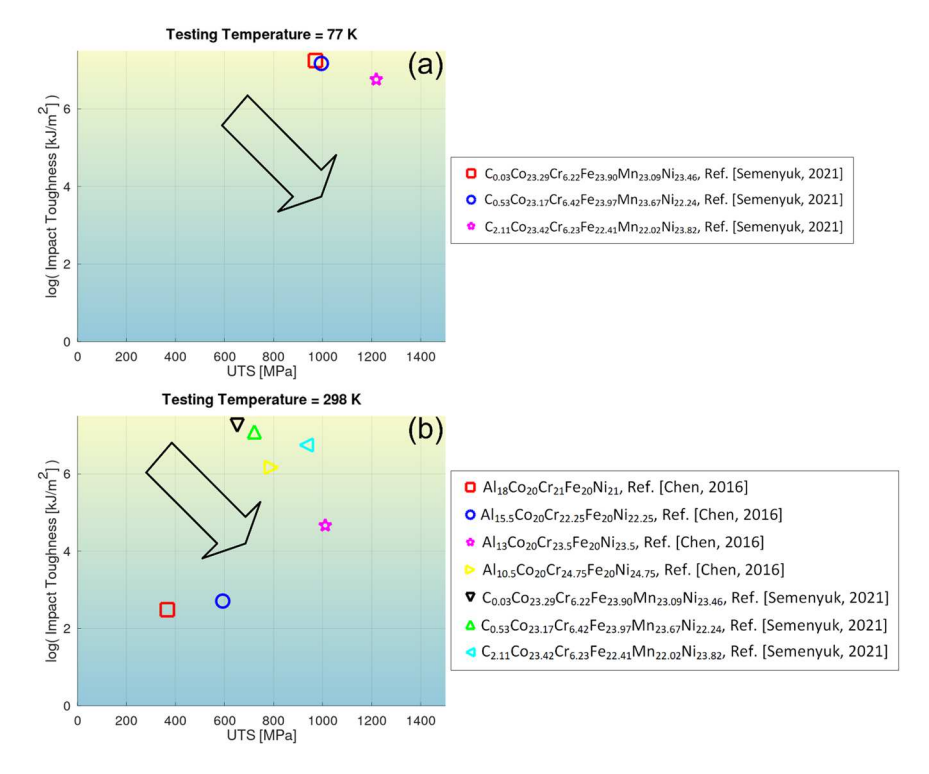


Fig. 5 Graphical compilation of impact toughness of high-entropy alloys as a function of their ultimate tensile strengths at the testing temperatures 63,72 . (a) $T = 77 \, \text{K}$. (b) $T = 298 \, \text{K}$. Note that only a fraction of data in the dataset with ultimate tensile strength available is plotted. The arrows in the graph indicate a trend.

record represents a uniquely defined metallurgical condition. In other words, one composition may correspond to multiple data records, but there must exist at least one other factor (e.g., grain size) distinguishing them from each other.

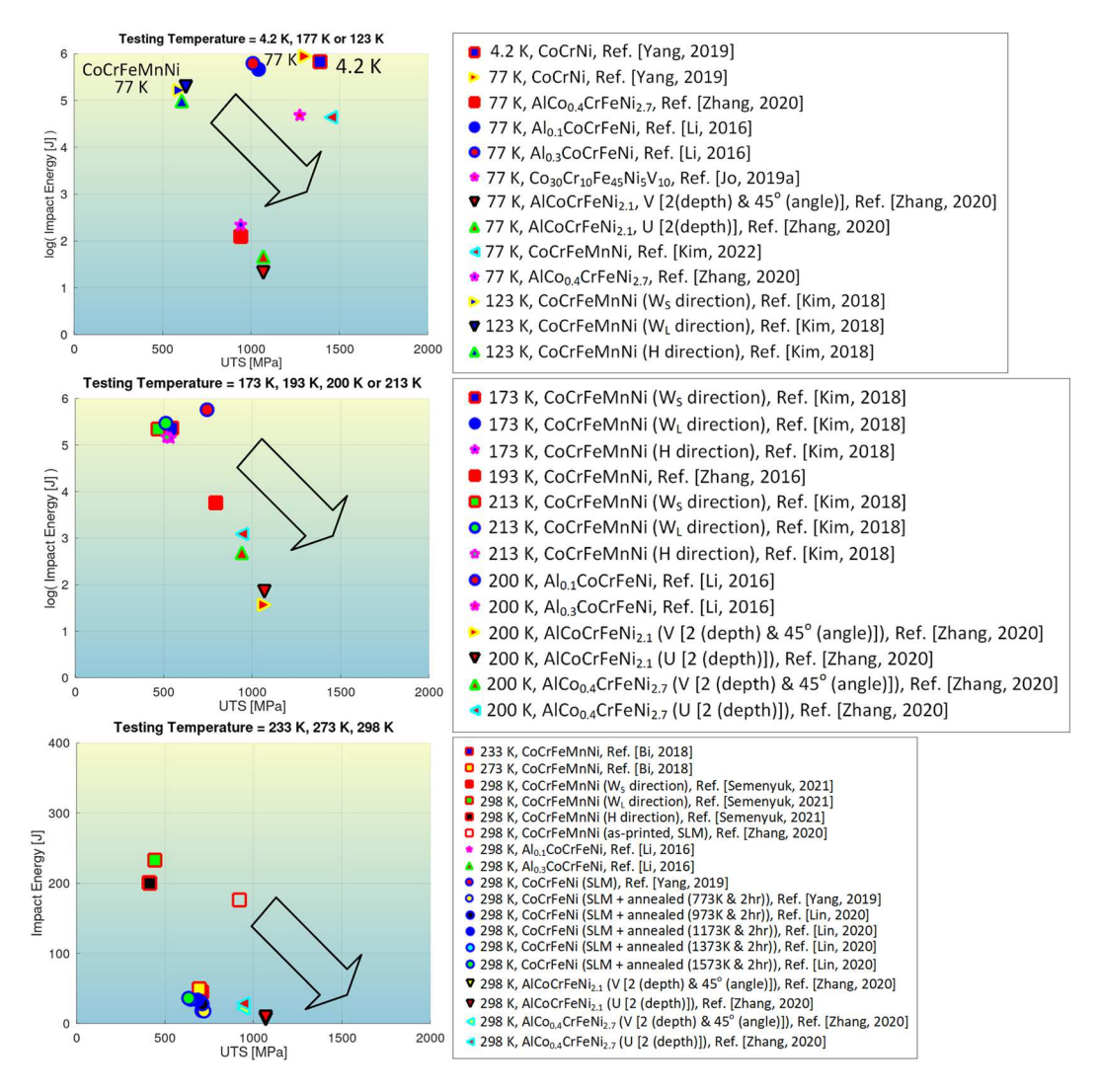


Fig. 6 Graphical compilation of data on impact energy of high-entropy alloys at the testing temperatures of $T = 4.2 \, \text{K}$, $T = 77 \, \text{K}$, $T = 123 \, \text{K}$, $T = 173 \, \text{K}$, $T = 193 \, \text{K}$, $T = 200 \, \text{K}$, $T = 213 \, \text{K}$, $T = 233 \, \text{K}$, $T = 273 \, \text{K}$ or $T = 298 \, \text{K}^{26,73-79}$. Note that only a fraction of data in the dataset with the ultimate tensile strength available is plotted. The arrows in the graph indicate a trend^{52,80-88}.

The data structure of the fracture toughness dataset is displayed in Fig. 2. It consists of over a dozen of blocks, with each block corresponding to a column in the Excel dataset. All the data blocks may be classified to several sub-groups, i.e., alloy basic information, tensile properties, fracture-toughness testing conditions, and the source reference, as signaled by differently colored blocks in Fig. 2. Impact toughness and impact energy data have similar data structures, as illustrated in Fig. 3.

Technical Validation

The original literature data of the same type coming in distinct units are converted to a consistent unit. The accuracy of the extracted data, derived data, and unit conversion is cross-checked and verified multiple times by the team.

Data visualization acts as an another means of data validation. All records in the individual datasets of fracture toughness, impact toughness, and impact energy are plotted to visually compare to the source plots in the literature from which the data are extracted. Any spotted discrepancies between our plots and the source ones are investigated and corrected if misrepresentation is confirmed.

Some of the plots in comparable conditions are given as follows. Figure 4 depicts the correlative plot between K_{IC} or K_Q of high-entropy alloys and the corresponding ultimate tensile strengths (UTS) at different testing temperatures. Likewise, the selected records in the impact toughness and impact-energy datasets are visualized in Figs. 5, 6, respectively. Note that Figs. 4–6 just account for a portion of the full data in the respective dataset where UTS of the alloys are available. The records without UTS availability are unplotted. The records not graphed yet covered in the dataset²⁸ are traced to refs. $^{31-60,80-88}$.

Usage Notes

The data contained in the dataset may be used individually or collectively for various purposes. The basic usage may involve comparing the fracture properties of individual HEAs in the dataset with other materials of interest or with HEAs later tested. Statistical analyses may also be collectively applied to the data to identify correlations or patterns between fracture indices and materials properties, such as the phase structure and grain size. As the database continues to grow, the data may be used for AI or machine learning to, for example, facilitate the design of highly fracture-resistant alloys⁶¹. Furthermore, many more usage possibilities are waiting to be explored by researchers.

Code availability

The code for digitizing the data from the literature plots is the open-source code WebPlotDigitizer version 4.5^{27} , which is freely accessible.

Received: 5 October 2022; Accepted: 15 December 2022; Published: 19 January 2023

References

- 1. Miracle, D. B. & Senkov, O. N. A critical review of high entropy alloys and related concepts. *Acta Mater.* 122, 448–511, https://doi.org/10.1016/j.actamat.2016.08.081 (2017).
- 2. Li, W. et al. Mechanical behavior of high-entropy alloys. Prog. Mater Sci. 118, 100777, https://doi.org/10.1016/j.pmatsci.2021.100777
- 3. Liaw, P. K. & Li, W. High entropy materials: Challenges and prospects. Metals 11, https://doi.org/10.3390/met11101643 (2021).
- 4. Yeh, J. W. et al. Nanostructured high-entropy alloys with multiple principal elements: Novel alloy design concepts and outcomes. *Adv. Eng. Mater.* **6**, 299–303, https://doi.org/10.1002/adem.200300567 (2004).
- 5. Cantor, B., Chang, I. T. H., Knight, P. & Vincent, A. J. B. Microstructural development in equiatomic multicomponent alloys. *Mater. Sci. Eng. A* 375–377, 213–218, https://doi.org/10.1016/j.msea.2003.10.257 (2004).
- Zhang, Y. et al. Microstructures and properties of high-entropy alloys. Prog. Mater Sci. 61, 1–93, https://doi.org/10.1016/j. pmatsci.2013.10.001 (2014).
- Tsai, K. Y., Tsai, M. H. & Yeh, J. W. Sluggish diffusion in Co-Cr-Fe-Mn-Ni high-entropy alloys. Acta Mater. 61, 4887-4897, https://doi.org/10.1016/j.actamat.2013.04.058 (2013).
- 8. Liu, X. et al. Enhancement of magnetic properties in FeCoNiCr0.4CuX high entropy alloys through the cocktail effect for megahertz electromagnetic wave absorption. J. Alloys Compd. 872, 159602, https://doi.org/10.1016/j.jallcom.2021.159602 (2021).
- 9. Lei, Z. et al. Enhanced strength and ductility in a high-entropy alloy via ordered oxygen complexes. Nature 563, 546–550, https://doi.org/10.1038/s41586-018-0685-y (2018).
- 10. Ding, Q. et al. Tuning element distribution, structure and properties by composition in high-entropy alloys. *Nature* **574**, 223–227, https://doi.org/10.1038/s41586-019-1617-1 (2019).
- nttps://doi.org/10.1036/841580-019-1617-1 (2019).

 11. Ma, E. Unusual dislocation behavior in high-entropy alloys. *Scripta Mater.* 181, 127–133, https://doi.org/10.1016/j.scriptamat. 2020.02.021 (2020).
- An, Z. et al. Hierarchical grain size and nanotwin gradient microstructure for improved mechanical properties of a non-equiatomic CoCrFeMnNi high-entropy alloy. J. Mater. Sci. Technol. 92, 195–207, https://doi.org/10.1016/j.jmst.2021.02.059 (2021).
- Zhang, Z. et al. Nanoscale origins of the damage tolerance of the high-entropy alloy CrMnFeCoNi. Nat. Commun. 6, 10143, https://doi.org/10.1038/ncomms10143 (2015).
- Li, Z., Pradeep, K. G., Deng, Y., Raabe, D. & Tasan, C. C. Metastable high-entropy dual-phase alloys overcome the strength–ductility trade-off. Nature 534, 227–230, https://doi.org/10.1038/nature17981 (2016).
- Li, W., Liaw, P. K. & Gao, Y. Fracture resistance of high entropy alloys: A review. Intermetallics 99, 69–83, https://doi.org/10.1016/j.intermet.2018.05.013 (2018).
- Li, W., Wang, G., Wu, S. & Liaw, P. K. Creep, fatigue, and fracture behavior of high-entropy alloys. J. Mater. Res. 33, 3011–3034, https://doi.org/10.1557/jmr.2018.191 (2018).
- Li, W., Chen, S. & Liaw, P. K. Discovery and design of fatigue-resistant high-entropy alloys. Scripta Mater. 187, 68–75, https://doi. org/10.1016/j.scriptamat.2020.05.047 (2020).
- Jia, H. et al. Fatigue and fracture behavior of bulk metallic glasses and their composites. Prog. Mater Sci. 98, 168–248, https://doi. org/10.1016/j.pmatsci.2018.07.002 (2018).
- 19. Anderson, T. L. Fracture mechanics: fundamentals and applications. (CRC press, 2017).
- 20. ASTM E399-17, Standard test method for linear-elastic plane-strain fracture toughness KIc of metallic materials. (ASTM International, 2017).
- 21. ASTM E1820-17, Standard test method for measurement of fracture toughness. (ASTM International, 2017).
- 22. ASTM E23-18, Standard Test Methods for Notched Bar Impact Testing of Metallic Materials. (ASTM International, 2018).
- 23. ASTM E2248-18, Standard Test Method for Impact Testing of Miniaturized Charpy V-notch Specimens. (ASTM International, 2018).
- 24. Zhang, H., He, Y. & Pan, Y. Enhanced hardness and fracture toughness of the laser-solidified FeCoNiCrCuTiMoAlSiB0.5 highentropy alloy by martensite strengthening. *Scripta Mater.* 69, 342–345, https://doi.org/10.1016/j.scriptamat.2013.05.020 (2013).
- 25. Roy, U., Roy, H., Daoud, H., Glatzel, U. & Ray, K. K. Fracture toughness and fracture micromechanism in a cast AlCoCrCuFeNi high entropy alloy system. *Mater. Lett.* 132, 186–189, https://doi.org/10.1016/j.matlet.2014.06.067 (2014).
- 26. Li, D. & Zhang, Y. The ultrahigh charpy impact toughness of forged AlxCoCrFeNi high entropy alloys at room and cryogenic temperatures. *Intermetallics* 70, 24–28, https://doi.org/10.1016/j.intermet.2015.11.002 (2016).
- 27. Rohatgi, A. Webplotdigitizer: Version 4.5, https://automeris.io/WebPlotDigitizer (2021).
- 28. X Fan, S Chen, B Steingrimsson, W Li, P K. Liaw, Dataset for fracture and impact toughness of high-entropy alloys, Materials Cloud Archive. https://doi.org/10.24435/materialscloud:d6-pf (2022).
- Chen, S., Fan, X., Li, W., Steingrimsson, B., Liaw, P.K. Fatigue database of high entropy alloys. Materials Cloud Archive https://doi. org/10.24435/materialscloud:s6-39 (2022).
- 30. Chen, S. et al. Fatigue dataset of high-entropy alloys. Scientific Data 9, 381, https://doi.org/10.1038/s41597-022-01368-5 (2022).
- Seifi, M., Li, D., Yong, Z., Liaw, P. K. & Lewandowski, J. J. Fracture Toughness and Fatigue Crack Growth Behavior of As-Cast High-Entropy Alloys. JOM 67, 2288–2295, https://doi.org/10.1007/s11837-015-1563-9 (2015).
- 32. Zou, Y. et al. Fracture properties of a refractory high-entropy alloy: In situ micro-cantilever and atom probe tomography studies. Scripta Mater. 128, 95–99, https://doi.org/10.1016/j.scriptamat.2016.09.036 (2017).
- 33. Mohanty, S. et al. Powder metallurgical processing of equiatomic AlCoCrFeNi high entropy alloy: Microstructure and mechanical properties. Mater. Sci. Eng. A 679, 299–313, https://doi.org/10.1016/j.msea.2016.09.062 (2017).
- 34. Luo, W., Liu, Y., Luo, Y. & Wu, M. Fabrication and characterization of WC-AlCoCrCuFeNi high-entropy alloy composites by spark plasma sintering. *J. Alloys Compd.* **754**, 163–170, https://doi.org/10.1016/j.jallcom.2018.04.270 (2018).
- 35. Wang, S.-P., Ma, E. & Xu, J. Notch fracture toughness of body-centered-cubic (TiZrNbTa)Mo high-entropy alloys. *Intermetallics* 103, 78–87, https://doi.org/10.1016/j.intermet.2018.10.008 (2018).

- 36. Chen, L. et al. Wear behavior of HVOF-sprayed Al0.6TiCrFeCoNi high entropy alloy coatings at different temperatures. Surf. Coat. Technol. 358, 215–222, https://doi.org/10.1016/j.surfcoat.2018.11.052 (2019).
- 37. Xiao, Y. et al. Nanostructured NbMoTaW high entropy alloy thin films: High strength and enhanced fracture toughness. Scripta Mater. 168, 51–55, https://doi.org/10.1016/j.scriptamat.2019.04.011 (2019).
- 38. Nair, R. B., Arora, H. S., Boyana, A. V., Saiteja, P. & Grewal, H. S. Tribological behavior of microwave synthesized high entropy alloy claddings. Wear 436-437, 203028, https://doi.org/10.1016/j.wear.2019.203028 (2019).
- Wang, Z. et al. The microstructure and properties of novel Ti(C,N)-based cermets with multi-component CoCrFeNiCu highentropy alloy binders. Mater. Sci. Eng. A 766, 138345, https://doi.org/10.1016/j.msea.2019.138345 (2019).
- 40. Fang, Y. et al. High-temperature oxidation resistance, mechanical and wear resistance properties of Ti(C,N)-based cermets with Al0.3CoCrFeNi high-entropy alloy as a metal binder. J. Alloys Compd. 815, 152486, https://doi.org/10.1016/j.jallcom.2019.152486 (2020).
- 41. Ganji, R. S., Rajulapati, K. V. & Rao, K. B. S. Development of a Multi-phase AlCuTaVW High-Entropy Alloy Using Powder Metallurgy Route and its Mechanical Properties. *Transactions of the Indian Institute of Metals* 73, 613–618, https://doi.org/10.1007/s12666-020-01875-2 (2020).
- 42. Long, Y., Che, J., Wu, Z., Lin, H.-T. & Zhang, F. High entropy alloy borides prepared by powder metallurgy process and the enhanced fracture toughness by addition of yttrium. *Mater. Chem. Phys.* 257, 123715, https://doi.org/10.1016/j.matchemphys.2020.123715 (2021).
- 43. Gou, Q. et al. Influence of NbC additions on microstructure and wear resistance of Ti(C,N)-based cermets bonded by CoCrFeNi high-entropy alloy. Int. J. Refract. Met. Hard Mater. 94, 105375, https://doi.org/10.1016/j.ijrmhm.2020.105375 (2021).
- 44. Erdogan, A., Günen, A., Gök, M. S. & Zeytin, S. Microstructure and mechanical properties of borided CoCrFeNiAl0.25Ti0.5 high entropy alloy produced by powder metallurgy. *Vacuum* 183, 109820, https://doi.org/10.1016/j.vacuum.2020.109820 (2021).
- Scales, R. J., Armstrong, D. E. J., Wilkinson, A. J. & Li, B. S. On the brittle-to-ductile transition of the as-cast TiVNbTa refractory high-entropy alloy. Materialia 14, 100940, https://doi.org/10.1016/j.mtla.2020.100940 (2020).
- Salemi, F., Karimzadeh, F. & Abbasi, M. H. Evaluation of Thermal and Mechanical Behavior of CuNiCoZnAl High-Entropy Alloy Fabricated Using Mechanical Alloying and Spark Plasma Sintering. *Metall. Mater. Trans. A* 52, 1947–1962, https://doi.org/10.1007/ s11661-021-06205-9 (2021).
- 47. Dada, M., Popoola, P., Mathe, N., Adeosun, S. & Pityana, S. Investigating the elastic modulus and hardness properties of a high entropy alloy coating using nanoindentation. *International Journal of Lightweight Materials and Manufacture* 4, 339–345, https://doi.org/10.1016/j.ijlmm.2021.04.002 (2021).
- 48. Liu, Q., Dong, T.-s, Fu, B.-g, Li, G.-l & Yang, L.-j Effect of Laser Remelting on Microstructure and Properties of AlCoCrFeNi High-Entropy Alloy Coating. J. Mater. Eng. Perform. 30, 5728–5735, https://doi.org/10.1007/s11665-021-05806-0 (2021).
- Günen, A. Tribocorrosion behavior of boronized Co1.19Cr1.86Fe1.30Mn1.39Ni1.05Al0.17B0.04 high entropy alloy. Surf. Coat. Technol. 421, 127426, https://doi.org/10.1016/j.surfcoat.2021.127426 (2021).
- 50. Górniewicz1a, D., Jóźwiak, S., Przygucki, H. & Kopec, M. The concept of improving the fracture toughness of double-phase high entropy alloy produced by high-pulse sintering method U-FAST.
- Solodkyi, I. et al. Hardmetals prepared from WC-W2C eutectic particles and AlCrFeCoNiV high entropy alloy as a binder. Vacuum 195, 110630, https://doi.org/10.1016/j.vacuum.2021.110630 (2022).
- 52. Jiang, H. et al. Design Multicomponent Eutectic Alloys in the Co-Cr-Fe-Ni-Nb System Using Simple Mixing Method. Adv. Eng. Mater. 24, 2101339, https://doi.org/10.1002/adem.202101339 (2022).
- 53. Hong, S., Li, J., Zhao, P., Xu, Y. & Li, W. Evolution in Wear and High-Temperature Oxidation Resistance of Laser-Clad AlxMoNbTa Refractory High-Entropy Alloys Coatings with Al Addition Content. *Coatings* 12, 121 (2022).
- Yang, S. et al. Effects of CrMnFeCoNi additions on microstructure, mechanical properties and wear resistance of Ti(C,N)-based cermets. J. Mater. Res. Technol. 17, 2480–2494, https://doi.org/10.1016/j.jmrt.2022.02.021 (2022).
- 55. Wu, Z., Chen, Y., Hai, W. & Liu, M. Effect of AlxCoCrFeNiCu binder on mechanical properties and wear performance of Ti(C, N) cermet. *Int. J. Mod Phys B* 36, 2240038, https://doi.org/10.1142/S0217979222400380 (2022).
- Zheng, D. High-Entropy-Alloy CoFeNiCr Bonded WC-Based Cemented Carbide Prepared by Spark Plasma Sintering. Metall. Mater. Trans. A 53, 2724–2729, https://doi.org/10.1007/s11661-022-06701-6 (2022).
- 57. Jiang, W. et al. Charpy impact behavior and deformation mechanisms of Cr26Mn20Fe20Co20Ni14 high-entropy alloy at ambient and cryogenic temperatures. *Mater. Sci. Eng. A* 837, 142735, https://doi.org/10.1016/j.msea.2022.142735 (2022).
- 58. Xia, S. Q., Gao, M. C. & Zhang, Y. Abnormal temperature dependence of impact toughness in AlxCoCrFeNi system high entropy alloys. *Mater. Chem. Phys.* 210, 213–221, https://doi.org/10.1016/j.matchemphys.2017.06.021 (2018).
- 59. Bi, G. et al. in Advanced Laser Processing and Manufacturing II. 43-52 (SPIE).
- 60. Ostovari Moghaddam, A., Pasandideh, J., Abdollahzadeh, A., Shaburova, N. A. & Trofimov, E. On the application of NbTaTiVW refractory high entropy alloy particles in the manufacturing process of WC based matrix body drill bits. *Int. J. Refract. Met. Hard Mater.* 99, 105608, https://doi.org/10.1016/j.ijrmhm.2021.105608 (2021).
- 61. Steingrimsson, B., Fan, X., Kulkarni, A., Gao, M. & Liaw, P. in High-entropy materials: Theory, experiments, and applications (eds J. Brechtl & P. K. Liaw) (Springer, 2021).
- 62. Gludovatz, B. et al. A fracture-resistant high-entropy alloy for cryogenic applications. Science 345, 1153–1158, https://doi.org/10.1126/science.1254581 (2014).
- 63. Chen, C., Pang, S., Cheng, Y. & Zhang, T. Microstructure and mechanical properties of Al20-xCr20+0.5xFe20Co20Ni20+0.5x high entropy alloys. J. Alloys Compd. 659, 279-287, https://doi.org/10.1016/j.jallcom.2015.10.258 (2016).
- Gludovatz, B. et al. Exceptional damage-tolerance of a medium-entropy alloy CrCoNi at cryogenic temperatures. Nat. Commun. 7, 10602, https://doi.org/10.1038/ncomms10602 (2016).
- Jo, Y. H. et al. Utilization of brittle σ phase for strengthening and strain hardening in ductile VCrFeNi high-entropy alloy. Mater. Sci. Eng. A 743, 665–674, https://doi.org/10.1016/j.msea.2018.11.136 (2019).
- Jo, Y. H. et al. Cryogenic-temperature fracture toughness analysis of non-equi-atomic V10Cr10Fe45Co20Ni15 high-entropy alloy. J. Alloys Compd. 809, 151864, https://doi.org/10.1016/j.jallcom.2019.151864 (2019).
- 67. Jo, Y. H. et al. Analysis of damage-tolerance of TRIP-assisted V10Cr10Fe45Co30Ni5 high-entropy alloy at room and cryogenic temperatures. J. Alloys Compd. 844, 156090, https://doi.org/10.1016/j.jallcom.2020.156090 (2020).
- Yang, J. et al. Effects of deformation-induced martensitic transformation on cryogenic fracture toughness for metastable Si8V2Fe45Cr10Mn5Co30 high-entropy alloy. Acta Mater. 225, 117568, https://doi.org/10.1016/j.actamat.2021.117568 (2022).
- 69. Fan, X. J., Qu, R. T. & Zhang, Z. F. Remarkably high fracture toughness of HfNbTaTiZr refractory high-entropy alloy. J. Mater. Sci. Technol. 123, 70–77, https://doi.org/10.1016/j.jmst.2022.01.017 (2022).
- 70. Liu, L.-X. et al. Achieving high strength and ductility in a 3D-printed high entropy alloy by cooperative planar slipping and stacking fault. Mater. Sci. Eng. A 843, 143106, https://doi.org/10.1016/j.msea.2022.143106 (2022).
- Liu, D. et al. Exceptional fracture toughness of CrCoNi-based medium- and high-entropy alloys at 20 kelvin. Science 378, 978–983, https://doi.org/10.1126/science.abp8070 (2022).
- 72. Semenyuk, A. et al. Effect of carbon content on cryogenic mechanical properties of CoCrFeMnNi high entropy alloy. IOP Conf. Ser. Mater. Sci. Eng. 1014, 012050, https://doi.org/10.1088/1757-899x/1014/1/012050 (2021).
- 73. Kim, J. H., Lim, K. R., Won, J. W., Na, Y. S. & Kim, H.-S. Mechanical properties and deformation twinning behavior of as-cast CoCrFeMnNi high-entropy alloy at low and high temperatures. *Mater. Sci. Eng. A* 712, 108–113, https://doi.org/10.1016/j.msea.2017.11.081 (2018).

- 74. Jo, Y. H. et al. Effects of deformation-induced BCC martensitic transformation and twinning on impact toughness and dynamic tensile response in metastable VCrFeCoNi high-entropy alloy. J. Alloys Compd. 785, 1056–1067, https://doi.org/10.1016/j.jallcom.2019.01.293 (2019).
- 75. Yang, M. et al. High impact toughness of CrCoNi medium-entropy alloy at liquid-helium temperature. Scripta Mater. 172, 66–71, https://doi.org/10.1016/j.scriptamat.2019.07.010 (2019).
- 76. Lin, D. et al. Effects of annealing on the structure and mechanical properties of FeCoCrNi high-entropy alloy fabricated via selective laser melting. Addit. Manuf. 32, 101058, https://doi.org/10.1016/j.addma.2020.101058 (2020).
- 77. Zhang, L. & Zhang, Y. Tensile properties and impact toughness of AlCoxCrFeNi3.1-x (x = 0.4, 1) high-entropy alloys. Front. Mater. Sci. 7, https://doi.org/10.3389/fmats.2020.00092 (2020).
- 78. Kim, Y.-K., Kim, M.-C. & Lee, K.-A. 1.45 GPa ultrastrong cryogenic strength with superior impact toughness in the *in-situ* nano oxide reinforced CrMnFeCoNi high-entropy alloy matrix nanocomposite manufactured by laser powder bed fusion. *J. Mater. Sci. Technol.* 97, 10–19, https://doi.org/10.1016/j.jmst.2021.04.030 (2022).
- 79. Bi, G. et al. in Advanced Laser Processing and Manufacturing II. 43-52 (SPIE).
- 80. Zhang, A., Han, J., Meng, J., Su, B. & Li, P. entropy alloy by spark plasma sintering from elemental powder mixture. *Mater. Lett.* 181, 82–85, https://doi.org/10.1016/j.matlet.2016.06.014 (2016).
- 81. Zhang, A., Han, J., Su, B., Li, P. & Meng, J. Microstructure, mechanical properties and tribological performance of CoCrFeNi high entropy alloy matrix self-lubricating composite. *Mater. Design* 114, 253–263, https://doi.org/10.1016/j.matdes.2016.11.072 (2017).
- 82. Li, N., Wu, S., Ouyang, D., Zhang, J. & Liu, L. Fe-based metallic glass reinforced FeCoCrNiMn high entropy alloy through selective laser melting. *J. Alloys Compd.* 822, 153695, https://doi.org/10.1016/j.jallcom.2020.153695 (2020).
- 83. Yadav, S., Sarkar, S., Aggarwal, A., Kumar, A. & Biswas, K. Wear and mechanical properties of novel (CuCrFeTiZn)100-xPbx high entropy alloy composite via mechanical alloying and spark plasma sintering. *Wear* 410-411, 93–109, https://doi.org/10.1016/j. wear.2018.05.023 (2018).
- 84. Zhang, A., Han, J., Su, B. & Meng, J. A promising new high temperature self-lubricating material: CoCrFeNiS0.5 high entropy alloy. *Mater. Sci. Eng. A* 731, 36–43, https://doi.org/10.1016/j.msea.2018.06.030 (2018).
- Chung, D., Ding, Z. & Yang, Y. Hierarchical Eutectic Structure Enabling Superior Fracture Toughness and Superb Strength in CoCrFeNiNb0.5 Eutectic High Entropy Alloy at Room Temperature. Adv. Eng. Mater. 21, 1801060, https://doi.org/10.1002/adem.201801060 (2019).
- 86. Xin, B., Zhang, A., Han, J., Su, B. & Meng, J. Tuning composition and microstructure by doping Ti and C for enhancing mechanical property and wear resistance of Al0.2Co1.5CrFeNi1.5Ti0.5 high entropy alloy matrix composites. *J. Alloys Compd.* 836, 155273, https://doi.org/10.1016/j.jallcom.2020.155273 (2020).
- 87. Guo, Z., Zhang, A., Han, J. & Meng, J. Microstructure, mechanical and tribological properties of CoCrFeNiMn high entropy alloy matrix composites with addition of Cr3C2. *Tribology International* 151, 106436, https://doi.org/10.1016/j.triboint.2020.106436 (2020).
- 88. Xin, B., Zhang, A., Han, J., Zhang, J. & Meng, J. Enhancing mechanical properties of the boron doped Al0.2Co1.5CrFeNi1.5Ti0.5 high entropy alloy via tuning composition and microstructure. *J. Alloys Compd.* 896, 162852, https://doi.org/10.1016/j.jallcom.2021.162852 (2022).

Acknowledgements

X. Fan and P. K. Liaw very much appreciate the supports from (1) the National Science Foundation (DMR-1611180, 1809640, and 2226508) with program directors, Drs. J. Madison, J. Yang, G. Shiflet, and D. Farkas, (2) the US Army Research Office (W911NF-13–1-0438 and W911NF-19–2-0049) with program managers, Drs. M.P. Bakas, S.N. Mathaudhu, and D.M. Stepp, and (3) the Paul and Madeline Bunch fellowship established by Mr. and Mrs. Bunch. BS very much appreciates the support from the National Science Foundation (IIP-1447395 and IIP-1632408), with the program directors, Dr. G. Larsen and R. Mehta, from the U.S. Air Force (FA864921P0754), with J. Evans as the program manager, and from the U.S. Navy (N6833521C0420), with Drs. D. Shifler and J. Wolk as the program managers.

Author contributions

X.S.F. and S.Y.C. extracted the data from the literature and constructed the dataset under the supervision of W.D.L. and P.K.L. B.S. made the plots. X.S.F., B.S., Q.G.X. and W.D.L. analyzed the data and wrote the manuscript. All authors contributed to data validation and manuscript reviewing. Correspondence should be addressed to W.D.L. or P.K.L.

Competing interests

The authors declare no competing interest.

Additional information

Correspondence and requests for materials should be addressed to W.L. or P.K.L.

Reprints and permissions information is available at www.nature.com/reprints.

Publisher's note Springer Nature remains neutral with regard to jurisdictional claims in published maps and institutional affiliations.

Open Access This article is licensed under a Creative Commons Attribution 4.0 International License, which permits use, sharing, adaptation, distribution and reproduction in any medium or format, as long as you give appropriate credit to the original author(s) and the source, provide a link to the Creative Commons license, and indicate if changes were made. The images or other third party material in this article are included in the article's Creative Commons license, unless indicated otherwise in a credit line to the material. If material is not included in the article's Creative Commons license and your intended use is not permitted by statutory regulation or exceeds the permitted use, you will need to obtain permission directly from the copyright holder. To view a copy of this license, visit https://creativecommons.org/licenses/by/4.0/.

This is a U.S. Government work and not under copyright protection in the US; foreign copyright protection may apply 2023